Multi-functional O_2-H_2 electrochemistry by an abundant mineral: A novel economical alternative for noble metals in electrolyzers and metal-air batteries

Zinoy Manappadan[a,b], Kaliaperumal Selvaraj[a,b,c*]

[a]*Nano and Computational Materials Lab., Catalysis and Inorganic Chemistry Division, CSIR-National Chemical Laboratory, Pune 411008, India*

[b]*Academy of Scientific and Innovative Research (AcSIR), Ghaziabad-201002, India*

[c]*Centre of Microscopy Facility, CSIR-National Chemical Laboratory, Pune 411008, India*

**Corresponding author: k.selvaraj@ncl.res.in, kselva@gmail.com*

Calculation of turnover frequency (TOF)

1. For OER

TOF for the OER is calculated for the four-electron pathway. The TOF can be calculated from the following equation [55]:

$$TOF\left(s^{-1}\right) = \frac{number\ of\ oxygen\ turnover\ per\ cm^2\ geometric\ area}{the\ active\ sites\ per\ \ cm^2\ geometric\ area}$$

$$TOF\left(s^{-1}\right) = \frac{number\ of\ oxygen\ turnover}{the\ active\ sites} = \frac{j/_{4F}}{m}$$

where j is the current density for OER at a given overpotential, F is Faraday constant (96485.3 As mol^{-1}), m is the number of moles of active sites, and (j/4F) represents the total oxygen turnover in OER.

The HAG catalyst loading on the carbon paper was 0.4 mg/cm^2. The TOF is calculated at the overpotential of 350 mV where the OER current is 21.33 mA cm^{-2} in 1 M KOH. An overpotential of 350 mV is selected for the TOF calculation for an easier comparison with the previously reported TOF values in the literature.

The number of oxygen turnover for OER is calculated from the current density according to the following equation:

$$N_{O2}(\frac{1}{cm^2 s}) = \frac{j(\frac{mA}{cm^2})}{1000} \text{ x } \frac{1\ mole\ e^-}{96485\ C} \text{ x} \frac{1\ mol\ O_2}{4\ mole\ e^-} \text{ x } 6.02\text{x } 10^{23} \text{x} \frac{1}{mol\ O_2}$$

Number of oxygen turnover for OER (j/4F) is then calculated as follows:

$$\frac{21.33\frac{mA}{cm^2}}{1000} \text{ x } \frac{1\ mole\ e^-}{96485\ C} \text{ x} \frac{1\ mol\ O_2}{4\ mole\ e^-} \text{ x } 6.02\text{x } 10^{23} = 3.3 \text{ x } 10^{16} \frac{1}{cm^2 s}$$

The percentage composition of HAG in the electrode ink is 80%. That makes 1.76 mg of HAG. Hence the active site density of Ca and P can be calculated using the equation

$$\frac{Mass\ loading \frac{mg}{cm^2} x\ Mass\ of\ species}{Molecular\ mass\ of\ species \frac{mg}{mol}} \text{x6.02x10}^{23}$$

Hence the active site density of Ca is

$$\frac{1.76 \frac{mg}{cm^2} x 0.57}{40.078 x\ 10^3 \frac{mg}{mol}} \text{x6.02x10}^{23} = 1.5 \text{ x } 10^{19} \text{ sites cm}^{-2}$$

The active site density of P is

$$\frac{1.76 \frac{mg}{cm^2} x 0.26}{30.974 x\ 10^3 \frac{mg}{mol}} \text{x6.02x10}^{23} = 9.3 \text{ x } 10^{18} \text{ sites cm}^{-2}$$

And thus, the TOF of Ca is calculated as below:

$$\text{TOF(s}^{-1}\text{) for OER} = \frac{3.3\ x\ 10^{16} (\frac{1}{cm^2 s})}{1.51\ x 10^{19} \frac{Sites}{cm^2}} = 2.2 \text{ x } 10^{-3} \text{ s}^{-1}$$

Similarly for P,

$$\text{TOF(s}^{-1}\text{) for OER} = \frac{3.3\ x\ 10^{16} (\frac{1}{cm^2 s})}{9.3\ x 10^{18} \frac{Sites}{cm^2}} = 3.5 \text{ x } 10^{-3} \text{ s}^{-1}$$

2. For HER

$$TOF\ (s^{-1}) = \frac{number\ of\ hydrogen\ turnover\ per\ cm^2\ geometric\ area}{the\ active\ sites\ per\ \ cm^2\ geometric\ area}$$

The TOF is calculated at the overpotential of 150 mV where the HER current is 131 mA cm^{-2} in 1 M KOH. As the mass loading is the same as in the case of OER, the active site density of Ca and P stays the same. The number of hydrogen turn over is calculated as,

$$N\ (H_2) = \frac{131\frac{mA}{cm^2}}{1000} \times \frac{1\ mole\ e^-}{96485\ C} \times \frac{1\ mol\ O_2}{2\ mole\ e^-} \times 6.02 \times 10^{23} = 1.02 \times 10^{17} \frac{1}{cm^2 s}$$

$$TOF\ of\ Ca = \frac{2.04}{40.078x\ 10^3 \frac{mg}{mol}} \times 10^{17} = 6.75 \times 10^{-3}\ s^{-1}$$

$$TOF\ of\ P = \frac{2.04}{40.078x\ 10^3 \frac{mg}{mol}} X\ 10^{17} = 1.1 \times 10^{-2}\ s^{-}$$

Calculation of mass activity

1. Mass activity for OER

Mass activity (A/mg) = j/m at 350 mV = 0.02133/2.2 = 9.7 x 10^{-3} A/mg

2. Mass activity for HER

Mass activity (A/mg) = j/m at 150 mV = 0.131/2.2 = 5.9 x 10^{-2} A/mg

3. Mass activity of ORR

Mass activity (A/mg) = j/m at 0.7 V = 0.41 x 10^{-3} /2 x 10^{-2} = 2.05 x 10^{-2} A/mg

Supplementary Figures

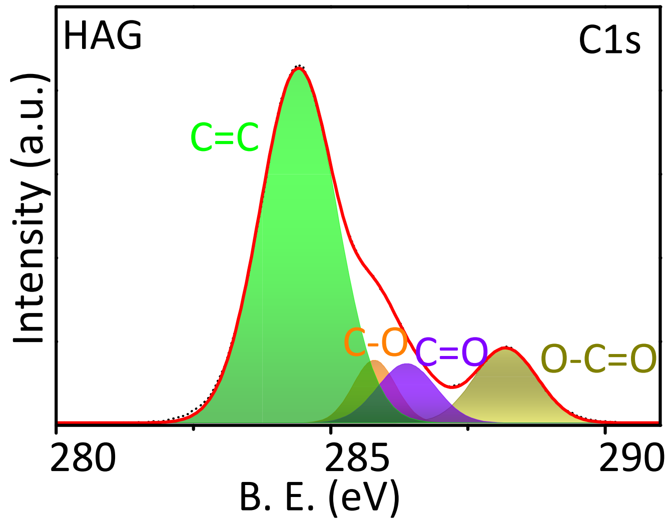

Figure S1: Core-level XPS spectra of C1s in HAG

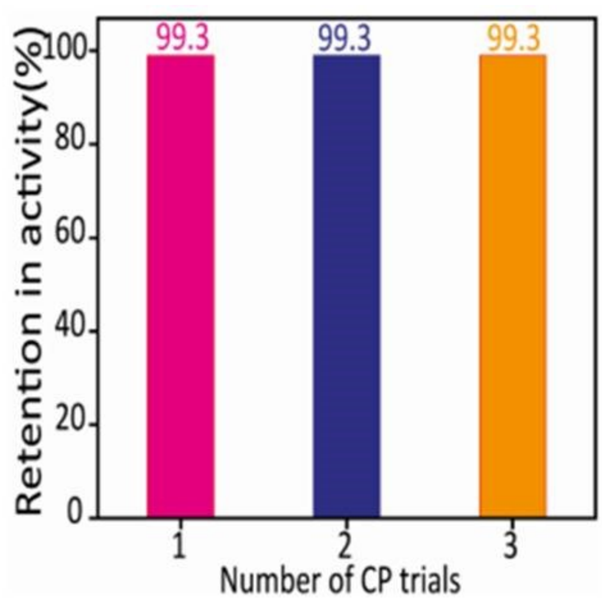

Figure S2: Retention of HER activity after each chronopotentiometric step

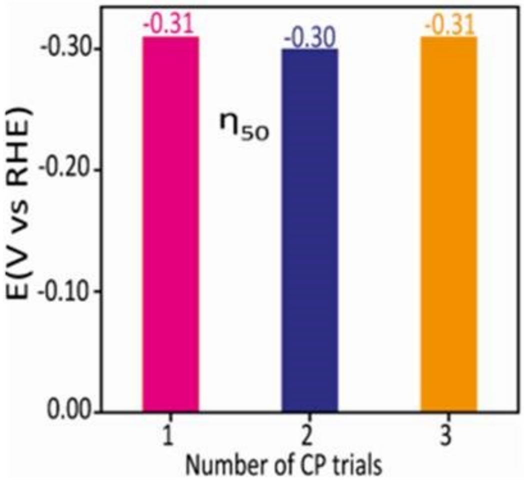

Figure S3: Comparison of η_{50} of the polarograms taken after each CP run.

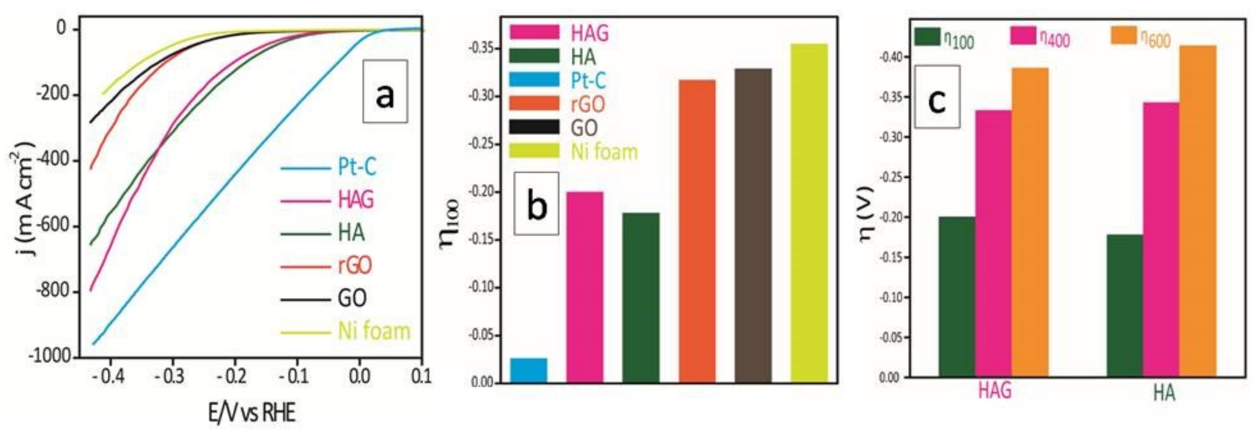

Figure S4: (a) Polarograms comparing the HER activity of Pt-C, HAG, HA, rGO, GO, and the Ni foam substrate (taken at 2 mV/ sec after 85 % iR compensation) (b) Bar diagram showing the η_{100} values of all the materials. (c) Bar diagram showing the $\eta_{100,}$ $\eta_{400,}$ η_{600}values of HA & HAG.

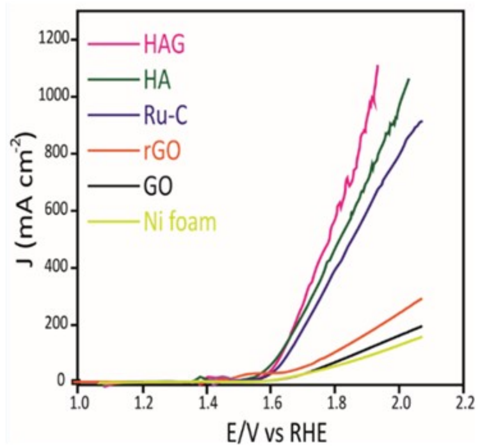

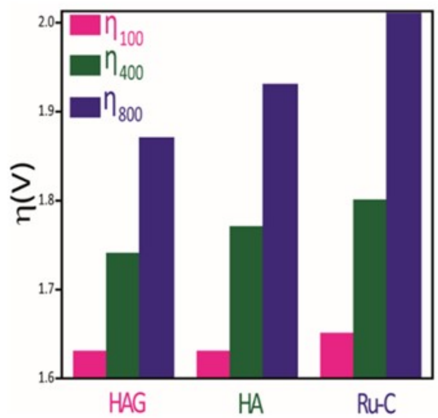

Figure S5: (a) Polarograms comparing the OER activity of Pt-C, HAG, HA, rGO, GO, and the Ni foam substrate (taken at 2 mV/ sec after 85 % iR compensation) (b) Bar diagram showing the $\eta_{100,}$ $\eta_{400,}$ η_{800} values of HA, HAG and Ru-C.

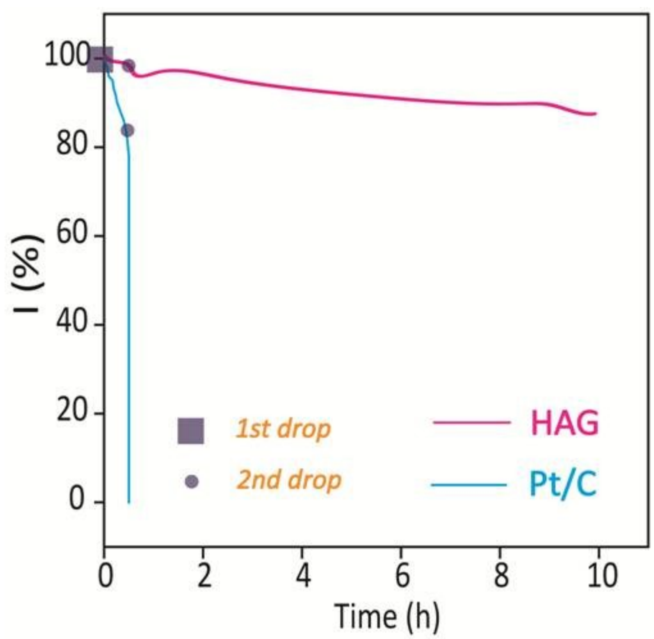

Figure S6: (a) Methanol poisoning test for HAG and Pt/C Supplementary Table

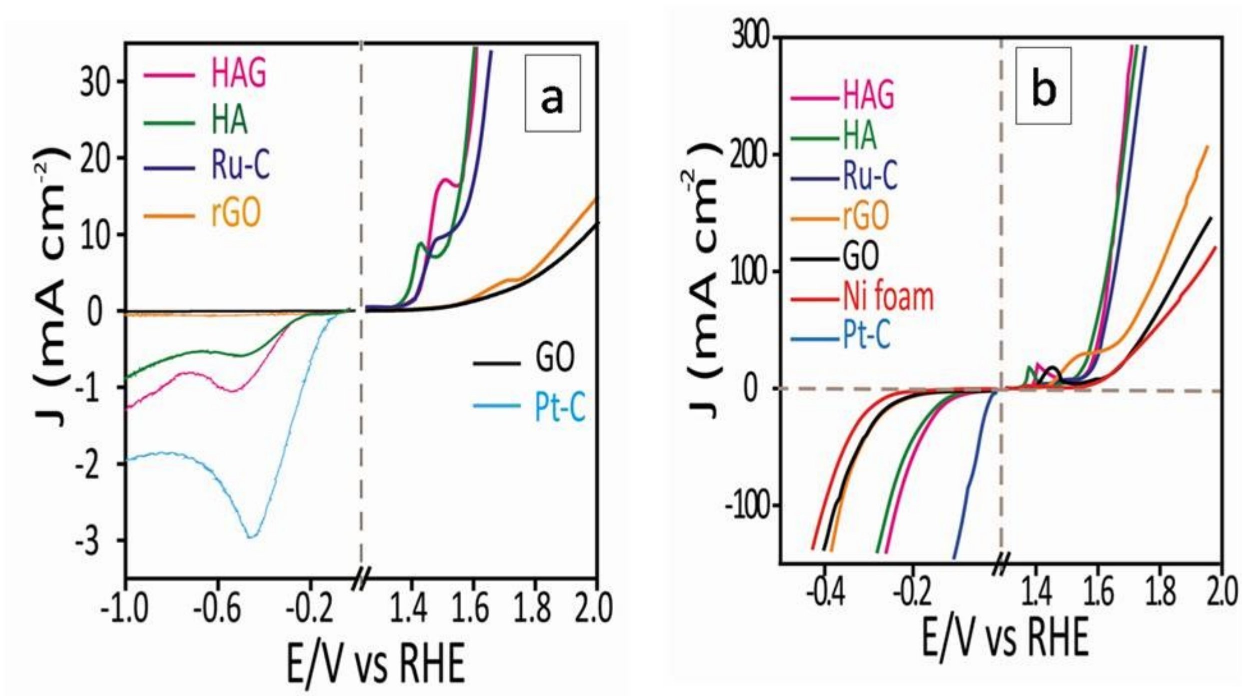

Figure S7: The bifunctional performance of HAG, HA, Ru-C, rGO and GO towards, (a) OER – ORR reaction pair and (b) OER - HER reaction pair.

Name	Peak BE	FWHM eV	Area (P) CPS.eV	Atomic %	Q
O 1*s*	537.33	2.93	2114470	52.03	1
Ca 2*p*	353.92	2.91	1492489	15.49	1
P 2*p*	140.01	2.96	297972	11.95	1
C 1*s*	291	6.64	345395.9	20.54	1

Table ST1: Quantitative elemental information from the XPS from where the Ca/P ratio was calculated (The rows containing the values of Ca and P are in highlights)

S No	Catalyst	Electrolyte	η_{10} HER (V)	η_{10} OER (V)	ΔE (V vs RHE)	Reference
1	Ni2P	1 M KOH	-0.220	1.52	1.74	S1
2	Co-P/NC	1 M KOH	-0.154	1.55	1.70	S2
3	NiCoP/rGO	1 M KOH	-0.209	1.5	1.71	S3
4	Ni3S2/NF	1 M KOH	-0.223	1.49	1.71	S4
5	Ni3FeN/r-GO-20	1 M KOH	-0.213	1.5	1.71	S5
6	Mo2C@CS	1 M KOH	-0.178	1.55	1.73	S6
7	Co4Mo2@NC/Ti	1 M KOH	-0.218	1.56	1.78	S7
8	CoOx@CN	1 M KOH	-0.232	1.49	1.72	S8
9	EG/Co0.85Se/NiFe-LDH	1 M KOH	-0.260	1.5	1.76	S9
10	CoMnO@CN	1 M KOH	-0.71	1.65	2.36	S10
11	EBP@NG	1 M KOH	-0.191	1.58	1.77	S11
12	ANSI	1 M KOH	-0.222	1.51	1.73	S12
13	NOGB	1 M KOH	-0.200	1.63	1.83	S13
14	NDCHN	1 M KOH	-0.201	1.52	1.72	S14
15	HAG/rGO	1 M KOH	-0.108	1.58	1.688	Present work

Table ST2: Summary of the HER and OER activities of recently reported bifunctional electrocatalysts for water splitting

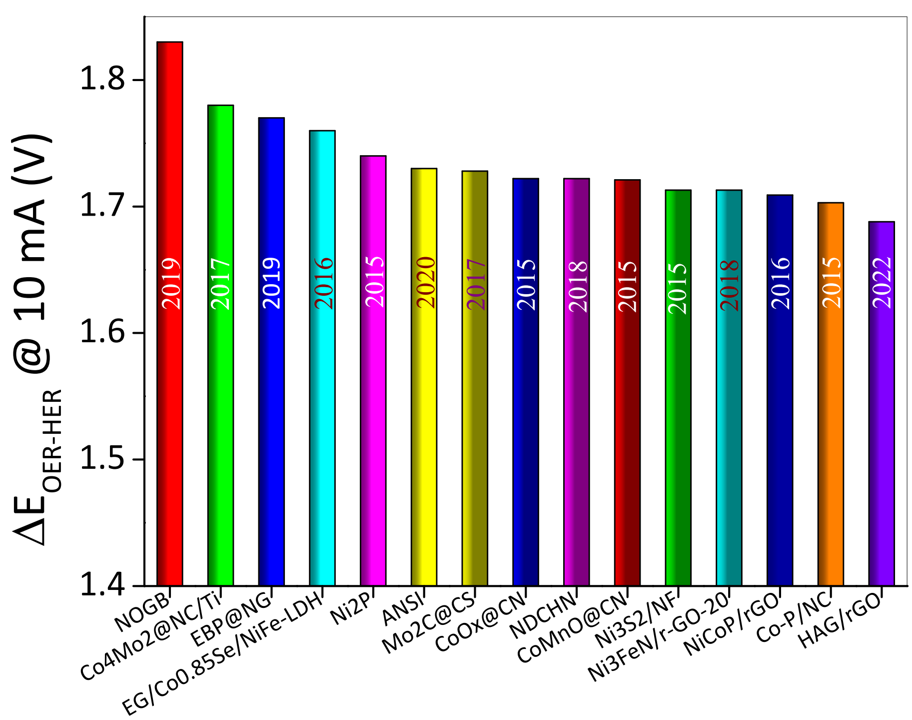

Figure S8: Bar diagram showing HAG over performing recently reported OER-HER bifunctional electrocatalysts

S No	Catalyst	Electrolyte	η_{10} OER (V vs RHE)	ORR $E_{1/2}$ (V vs RHE)	$\Delta E = \eta_{10} - E_{1/2}$ (V)	Reference
1	NCNF-1000	1M KOH	1.84	0.82	1.02	S15
2	P-gC_3N_4	1M KOH	1.63	0.67	0.96	S16
3	Mn oxide film	1 M KOH	1.77	0.73	1.04	S17
4	Fe@N-C	1 M KOH	1.71	0.83	0.88	S18
5	N-graphene CNT	1 M KOH	1.63	0.63	1	S19
6	Co_3O_4/Co_2MnO_4	1 M KOH	1.77	0.68	1.09	S20
7	Mn_xO_y/N-C	1 M KOH	1.68	0.81	0.87	S21
8	$LiCoO_2$	0.1 M KOH	1.67	0.70	0.97	S22
9	N-MWCNT	0.1 M KOH	0.75 (SCE)	-0.3 (SCE)	1.05	S23
10	HAG	0.1 M KOH	1.58	0.74	0.84	Present work

Table ST3: Summary of the ORR and OER activities of recently reported bifunctional electrocatalysts for water splitting

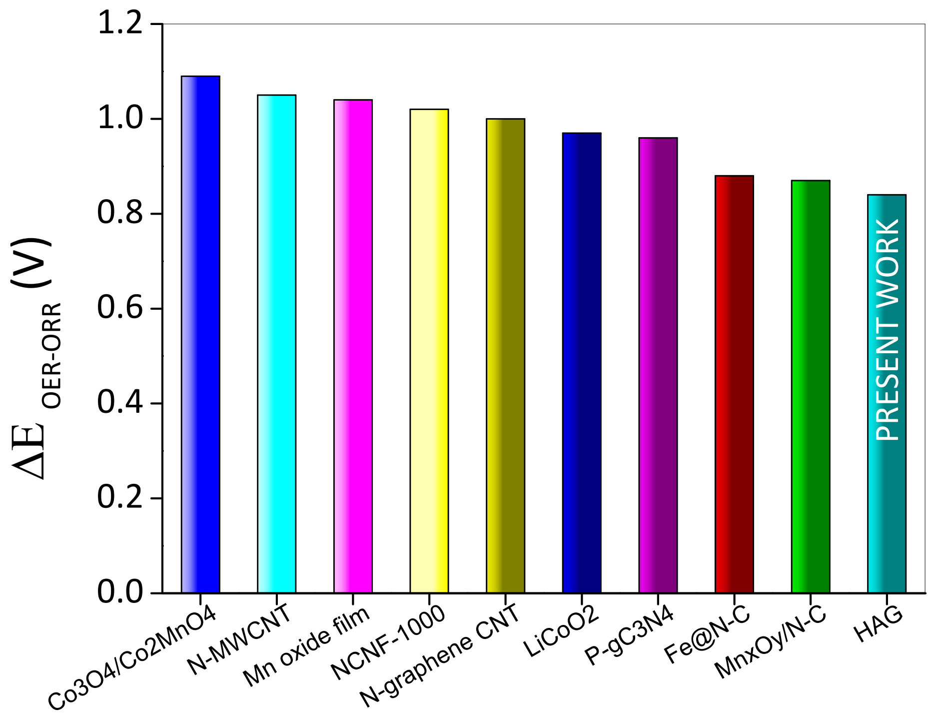

Figure S9: Bar diagram showing HAG over performing recently reported OER-ORR bifunctional electrocatalysts

References

S1. L.-A. Stern, L. Feng, F. Song and X. Hu, Energy Environ. Sci., 2015, 8, 2347-2351

S2. B. You, N. Jiang, M. Sheng, S. Gul, J. Yano and Y. Sun, Chem. Mater., 2015, 27, 7636- 7642

S3. J. Li, M. Yan, X. Zhou, Z. Q. Huang, Z. Xia, C. R. Chang, Y. Ma and Y. Qu, Adv. Funct. Mater., 2016, 26, 6785-6796

S4. L.-L. Feng, G. Yu, Y. Wu, G.-D. Li, H. Li, Y. Sun, T. Asefa, W. Chen and X. Zou, J. Am. Chem. Soc., 2015, 137, 14023-14026

S5. Y. Gu, S. Chen, J. Ren, Y. A. Jia, C. Chen, S. Komarneni, D. Yang and X. Yao, ACS Nano, 2018, 12, 245-253

S6. H. Wang, Y. Cao, C. Sun, G. Zou, J. Huang, X. Kuai, J. Zhao and L. Gao, ChemSusChem, 2017, 10, 3540-3546

S7. J. Jiang, Q. Liu, C. Zeng and L. Ai, J. Mater. Chem. A, 2017, 5, 16929-16935

S8. H. Jin, J. Wang, D. Su, Z. Wei, Z. Pang and Y. Wang, J. Am. Chem. Soc., 2015, 137, 2688-2694

S9. Y. Hou, M. R. Lohe, J. Zhang, S. Liu, X. Zhuang and X. Feng, Energy Environ. Sci., 2016, 9, 478–483

S10. J. Li, Y. Wang, T. Zhou, H. Zhang, X. Sun, J. Tang, L. Zhang, A. M. Al-Enizi, Z. Yang and G. Zheng, J. Am. Chem. Soc., 2015, 137, 14305–14312

S11. Zhongke Yuan, Jing Li, Meijia Yang, Zhengsong Fang, Junhua Jian, Dingshan Yu, Xudong Chen, Liming Dai, : J. Am. Chem. Soc. 2019, 141, 4972−4979

S12. Li X, Xu Y, Li Y, Fan X, Zhang G, Zhang F, et al. Increasing the heteroatoms doping percentages of graphene by porous engineering for enhanced electrocatalytic activities. J Colloid Interface Sci 2020;577:101e8

S13. Hu Q, Li G, Li G, Liu X, Zhu B, Chai X, et al. Trifunctional electrocatalysis on dual-doped graphene nanoringseintegrated boxes for efficient water splitting and ZneAir batteries. Adv Energy Mater 2019;9

S14. Zhang L, Hu JS, Huang XH, Song J, Lu SY. Particle-in-box nanostructured materials created via spatially confined pyrolysis as high performance bifunctional catalysts for electrochemical overall water splitting. Nano Energy 2018;48:489e99

S15. Qin Liu , Yaobing Wang , Liming Dai , Jiannian Yao, Scalable Fabrication of Nanoporous Carbon Fiber Films as Bifunctional Catalytic Electrodes for Flexible Zn-Air Batteries, Adv. Mater. 2016, 28, 3000–3006

S16. T. Y. Ma , J. Ran , S. Dai , M. Jaroniec , S. Z. Qiao , Angew. Chem. 2015 , 127 , 4729

S17. Y. Gorlin , T. F. Jaramillo , J. Am. Chem. Soc. 2010 , 132 , 13612

S18. J. Wang, H. Wu, D. Gao, S. Miao, G. Wang, X. Bao, Nano Energy 2015, 13, 387-396

S19. G. L. Tian, M. Q. Zhao, D. Yu, X.Y. Kong, J. Q. Huang, Q. Zhang, F. Wei, Small 2015, 10, 2251-2259

S20. J. Masa, W. Xia, I. Sinev, A. Zhao, Z. Sun, S. Grützke, P. Weide, M. Muhler, W. Schuhmann, Angew. Chem. Int. Ed. 2014, 53, 8508–8512

S21. D. U. Lee, J.-Y. Choi, K. Feng, H. W. Park, Z. Chen, Adv. Energy Mater. 2014, DOI: 10.1002/aenm.201301389

S22. Maiyalagan, T., Jarvis, K., Therese, S. *et al.* Spinel-type lithium cobalt oxide as a bifunctional electrocatalyst for the oxygen evolution and oxygen reduction reactions. *Nat Commun* **5**, 3949 (2014)

S23. Gui-Li Tian , Qiang Zhang , Bingsen Zhang , Yu-Guang Jin , Jia-Qi Huang , Dang Sheng Su , Fei Wei, Toward Full Exposure of "Active Sites": Nanocarbon Electrocatalyst with Surface Enriched Nitrogen for Superior Oxygen Reduction and Evolution Reactivity, Adv. Funct. Mater. 2014, 24, 5956–5961